

# Silicon Strips and Pixel Technologies

## Hand-on: Pixel systems at the LHC

### Objective

Get familiar with the general pixel detector design by comparing exhibited modules from different experiments. Understand the handling of pixel detectors on the example of the current ATLAS n-in-n pixel detector by performing the main front-end tuning steps as well as source measurements with radioactive  $^{241}\text{Am}$ .

### Introduction

The basic goal of the ATLAS Pixel Detector is to provide three high resolution space points. The sensitive part of the detector is about 1.3 m long, 35 cm in diameter and has a weight of 4.4 kg. It consists of three coaxial cylindrical barrel layers with nominal radii of 50.5, 88.5 and 122.5 mm. The global core support structure is locating three layers, holding 22, 38 and 52 structural elements, so-called staves. Each stave supports 13 pixel modules which mean that the 112 staves in the detector are holding 1456 pixel modules. Including the disks at both sides of the experiment, it comprises 1744 pixel modules

### ATLAS pixel module

The ATLAS pixel module consists of three main parts: The n-in-n pixel sensor, 16 FE-I3 front-end chips and the so-called flex hybrid, which is loaded with different electronic components.

The flex hybrid provides the necessary means to establish the communication between the front-end electronic chips with the outside of the experiment by a Module Control Chip as well as supply voltages for the front-end electronic and the bias voltage for the sensor.

In each module more than 46,000 electrical connections have to be realized between the sensor and the 16 FEs. Each connection between a sensor pixel and its FE readout channel is made through a bump bond with a minimal pitch between two connections of 50  $\mu\text{m}$ . These bump bonds are also the only mechanical interface between the sensor and the front-end chips.

### ATLAS front-end chip (FE-I3)

In order to measure the amount of charge deposited in each pixel, this information needs to be digitized by the front-end electronic. In the ATLAS experiment the FE-I3 chip with its

roughly 3.5 M transistors is taking care of this task. Each chip has  $18 \times 160 = 2880$  pixel readout cells which are covering an active area of the sensor tile of  $7.2 \times 10.8 \text{ mm}^2$

Figure 1 shows the three functional sections of a FE-I3 chip. The biggest part of the chip is used by a matrix of 2880 readout channels. The middle part, so-called bottom of column region, contains the end of column logic and Level 1 Trigger buffers and the bottom part of the chip contains the data serializers and the pad frame.

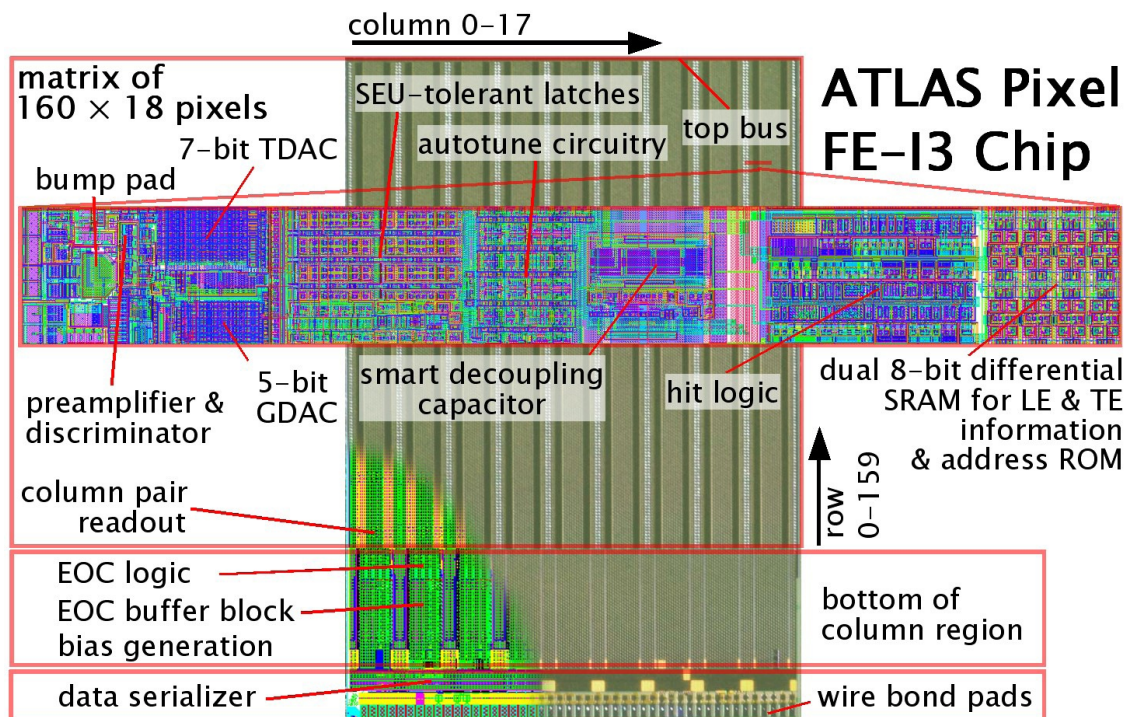


Figure 1: Layout of the ATLAS Pixel FE chip and a single pixel channel

The dimensions of a FE pixel cell correspond to the sensor pixel dimensions of  $50 \times 400 \mu\text{m}^2$ . FE channels incorporate a fast preamplifier with a feedback capacitance, a DC-coupled second stage and a fast differential discriminator. Eleven 8-bit current mode DACs, are used to control the biasing of critical nodes in the preamplifier and the discriminator, as well as threshold adjustment of the discriminator.

Figure 2 shows the block diagram and digital readout of a pixel cell. The bump bond pad in the left connects the sensor pixel with the preamplifier. A 3-bit local DAC (FDAC) allows for separately regulation of the feedback current of each pixel, whereas the bias current IF is used to globally adjust the feedback current for all pixels. The feedback capacitor is discharged by the constant current so that a triangular pulse shape is obtained.

The second stage differential pair amplifier and the discriminator follow the preamplifier. A 5-bit DAC (GDAC), allows to adjust the overall threshold for a FE very linear and fine-grained. A 6-bit local DAC (TDAC) in each pixel (a 7th bit is used to choose in which of the two nodes to inject the current) is used to increase the threshold of a pixel with about 75 e<sup>-</sup> per DAC count in the mid-range. These local trim bits affect both sides of the differential pair amplifier, resulting in a linear threshold vs. DAC behavior. The threshold can be varied from 0 to about 1 fC. The normal operation threshold is about 0.7 fC or 4 ke<sup>-</sup> equivalents.

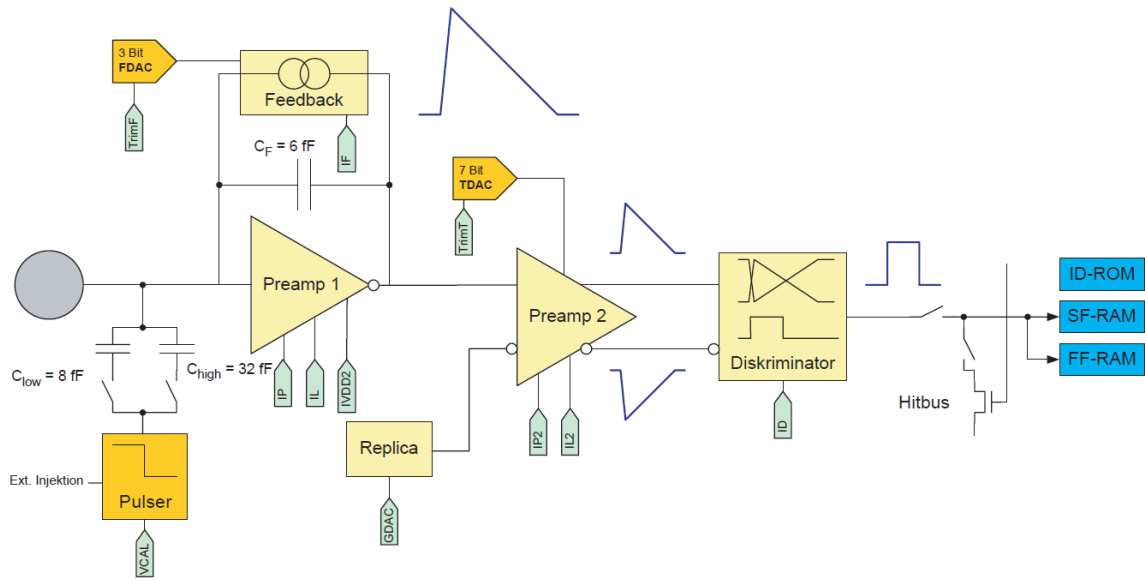
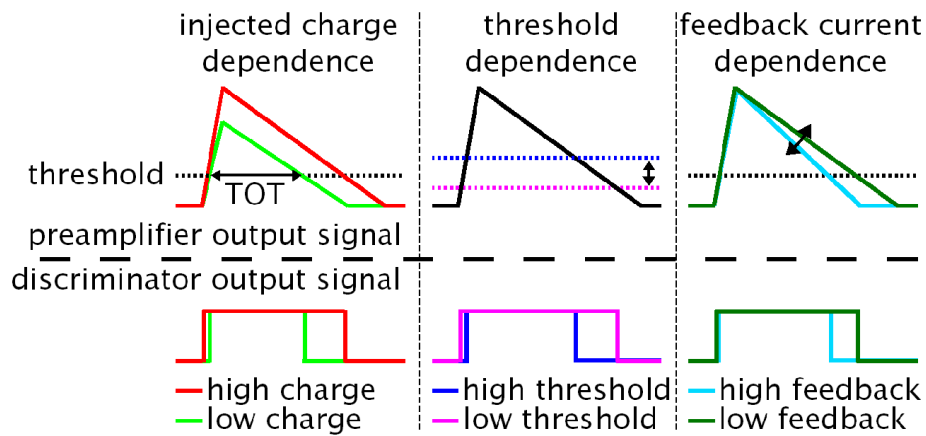


Figure 2: Block diagram of the FE pixel cell

Due to the linear discharge of the feedback current it is proportional to the deposited charge in the sensor. The feedback is adjusted so that it is a good compromise between high Time-over-Threshold (ToT) resolution and a small pixel dead time.

The connection between preamplifier and discriminator output signal shape as well as the dependence of the threshold and feedback current are shown in Figure 3.



### Preamplifier and Discriminator Signal Shapes

Figure 3: Injected charge, threshold and feedback current dependences of the TOT in the FE

An analogue injection circuit is implemented in each pixel to test the pixel readout cell, tune the threshold and calibrate ToT. Either direct pulses on the external Ext.Injection line can enter into the capacitors or a voltage step is generated by using the VCAL, which is a voltage provided by a DAC in the bottom of column region.

To measure the deposited charge of a hit the TOT for the discriminator output pulse is measured in units of the 40 MHz crossing clock.

## ATLAS pixel sensor

The ATLAS Pixel sensor has an active area of  $16.4 \times 60.8 \text{ mm}^2$  with a pixel size which is corresponding to the front-end chip  $50 \times 400 \mu\text{m}^2$ . High demands on production quality are necessary to achieve an acceptable production yield. Additional challenges, compared to industrial microchip production, are the required high purity of the silicon, the structuring of the wafer from both sides and the required radiation hardness of the sensor.

On one hand the sensor needs to be thick enough to obtain a high charge signal to be easily detected by the FE electronics and have a high signal-to-noise ratio (SNR). On the other hand it should be as thin as possible to minimize multiple scattering in the pixel detector. A compromise between these two demands is the used sensor thickness of  $250 \mu\text{m}$ . It leads to a mean MIP signal of about 25 k electrons.

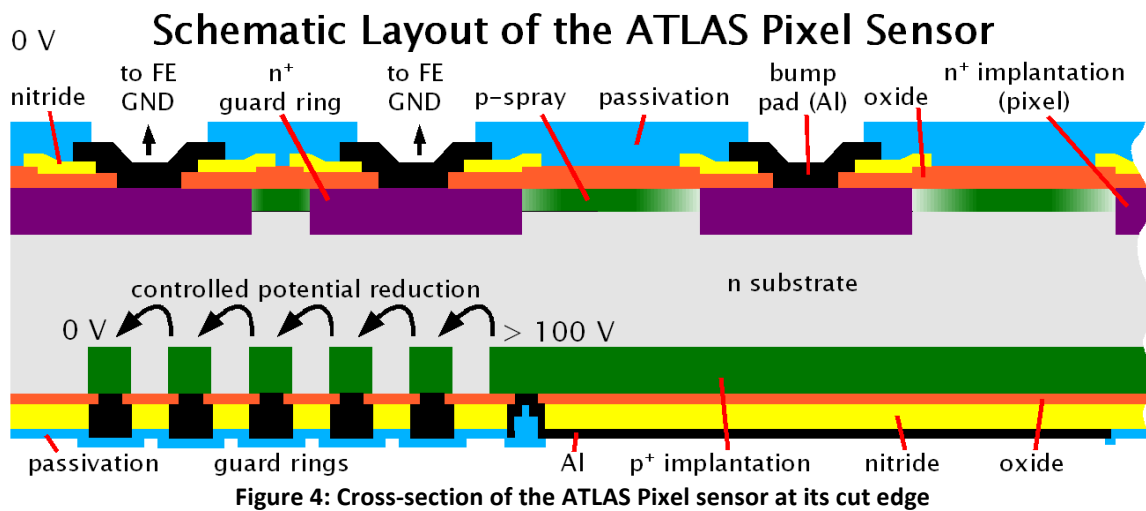


Figure 4: Cross-section of the ATLAS Pixel sensor at its cut edge

The bias voltage is connected to the p+ implantation, thus the n-side of the sensor has ground potential. This is important for hybrid pixel detectors, since a potential difference between the sensor and the FEs could lead to a flashover in the  $25 \mu\text{m}$  gap. A flashover could also happen at the edge of the sensor, if the pn junction on the p-side reaches the cut edge of the sensor. Thus a multi guard ring structure, metalized isolated floating p+ implantations, is implemented around the main p+ implantation close to the edge of the sensor to lower the bias potential step by step to zero. It also prevents the depletion zone from reaching the cut edge of the sensor, where crystal defects would inject charge carriers to the bulk and therefore increase the leakage current. A cross-section of the guard rings and the controlled potential reduction is shown in the lower left corner of Figure 4.

# Measurements

## Front-end tuning

### Digital Test:

During the Digital Test, for each pixel, pulses are injected at the output of the discriminator in order to simulating the discriminator signal when a preamplifier pulse triggers the discriminator. This part of the test checks all the readout chain from the pixel cell down to event building.

**Questions:** What are possible reasons for “dead” pixels on the digital level? What are the next testing steps in the detector quality assurance procedure?

### Threshold Scan:

A voltage pulse generated by an on-chip chopper connected to VCAL, is injected on the calibration capacitance  $C_{low}$  of each pixel. This will generate a signal at the input of the preamplifier equivalent to charge generated by a particle passing the pixel.

A set of pulses is generated for different value of the injected charge (from 0 to ~9000 electron, in ~45 electron steps).

The number of collected hits for each injected charge is recorded and at the end of the scan an S-curve is fitted. The 50% efficiency on the S-curve defines the threshold value. The steepness of the transition from no detected hits to full efficiency is inversely proportional to the noise, which can be calculated with this measurement results.

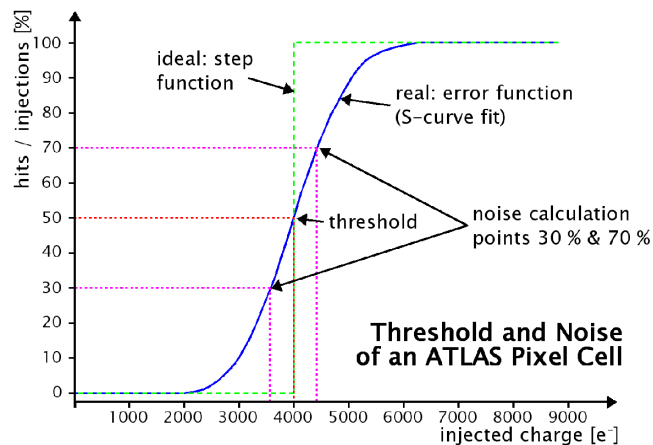


Figure 5: Schematic result of a Pixel cell threshold scan with the ideal step function and real error

**Questions:** What is the obtained threshold, noise and threshold dispersion? What are reasons that different pixels have per se (before tuning) a different threshold? Why is tuning necessary?

### Time-over Threshold calibration:

At first, the ToT response of all pixels to the charge deposited by a MIP is made uniform by a proper setting of the IF and FDAC values. This is done by injecting a fixed charge and choosing the above mentioned DACs in order to receive the desired average ToT response.

The subsequent step is to inject different charges, compute the average ToT observed for each pixel and each charge, and fit a calibration function to these data, in order to receive the fit parameter to convert a ToT value to a charge.

$$ToT = A + \frac{B}{C + Q_{inj}}$$

**Questions:** Why is the Time-over Threshold calibration necessary? Shouldn't be the threshold tuning be sufficient?

### **Source scan**

The main point of this test is to obtain the characteristic photoelectric peak of a  $^{241}\text{Am}$  source, thereby having a proof of the correct working condition and calibration of the detectors.  $^{241}\text{Am}$  gamma source emits 60 keV photons, which can convert anywhere in the bulk to a 60 keV primary electron. If ionization takes place in the substrate region where columns overlap, a signal of  $16.5\text{ke}^-$  is expected. On the other hand, if a photon converts in a high doping region or close to the surfaces, a fraction of the charge could be lost. Thus, in the charge distribution, a high end peak at  $16.5\text{ke}^-$  and a tail towards smaller values are expected.

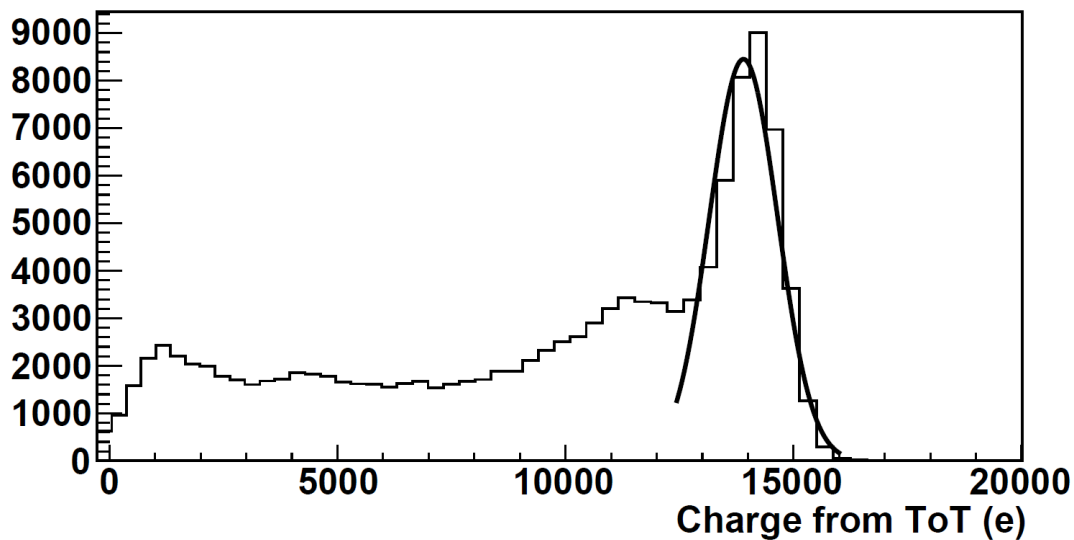


Figure 6: Photoelectric peak of a source measurement with  $^{241}\text{Am}$

**Questions:** What are additional reasons to see deposited charge below the photoelectric peak? How is this improved in an experiment? Why is a signal of  $16.5\text{ke}^-$  expected using a 60 KeV  $^{241}\text{Am}$  source?